# Heavy-quarkonium systems and the QCD scale parameter $\Lambda_{\overline{\rm MS}}$

Keiji Igi
*Department of Physics, University of Tokyo, Bunkyo-ku, Tokyo 113, Japan*

Seiji Ono*
*Institute of Physics, University of Tokyo, Komaba, Meguro-ku, Tokyo 153, Japan*
(Received 7 February 1986)

We study how the properties of $t$-quarkonium states depend on the scale parameter $\Lambda_{\overline{\rm MS}}$, where $\overline{\rm MS}$ is the modified minimal subtraction scheme. We find that if $\Lambda_{\overline{\rm MS}}$ is as small as 100 MeV the shape of the $Q\bar{Q}$ potential for the low-lying $t\bar{t}$ states with $m_t \sim 40$ GeV is already almost uniquely determined while if $\Lambda_{\overline{\rm MS}}$ is as large as 500 MeV the ambiguity in $E(2S)-E(1S)$, e.g., becomes much larger ($\sim 20\%$). We also study the difference of predictions of $t$-quarkonium spectra between nonrelativistic and relativistic models. Finally we show that hyperfine and fine splittings are sensitive to the value of $\Lambda_{\overline{\rm MS}}$, and hence the allowed range of $\Lambda_{\overline{\rm MS}}$ may be restricted from the data of already known quarkonia, $c\bar{c}$ and $b\bar{b}$.

## I. INTRODUCTION

Heavy-quark systems have a very clean spectroscopy which allows precision measurements of all the basic properties of the states. Up to the present, various particles which contain the $b$ quark, e.g., $\Upsilon$, $\Upsilon'$, . . . , $B$,$B^*$ are already found (see, e.g., Refs. 1 and 2), and the UA1 Collaboration[3] at the CERN $\bar{p}p$ collider seems to find events which are consistent with the top quark having a mass between 30 and 50 GeV. In the near future the energy region accessible for the $e^+e^-$ colliding machine will be increased drastically and we can expect that the $t$-quarkonium states will be found and studied in detail.

The properties of $t$-quarkonium states have been studied theoretically by various authors (see, e.g., Refs. 4–11). Because of the success of the nonrelativistic potential model and the flavor independence of the $Q\bar{Q}$ potential, we can say that the shape of the potential between 0.1 and 1 fm is already fixed. The root-mean-square radius of the $t\bar{t}$ ground state becomes substantially smaller than those of the $c\bar{c}$ and $b\bar{b}$ states due to the large top-quark mass, and hence it will be able to distinguish between various kinds of potentials as well as different values of $\Lambda_{\overline{\rm MS}}$, where $\overline{\rm MS}$ stands for the modified minimal subtraction scheme.

In Sec. II we find various $Q\bar{Q}$ potentials which are consistent with QCD expectation and reproduce $c\bar{c}$ and $b\bar{b}$ properties using the Schrödinger equation. In Sec. III we use the Salpeter equation in order to study the relativistic effects to heavy-quarkonium spectra. Adopting these potentials we study properties of the $t\bar{t}$ states as a function of $\Lambda_{\overline{\rm MS}}$ and show the theoretical ambiguities in Sec. IV. In order to see the allowed range of $\Lambda_{\overline{\rm MS}}$ in our model we also compute spin-dependent forces of $c\bar{c}$ and $b\bar{b}$ states as a function of $\Lambda_{\overline{\rm MS}}$ and compare them with the data in Sec. V. Summary and conclusions are presented in Sec. VI.

## II. THE $Q\bar{Q}$ POTENTIAL

Some time ago, Buchmüller and Tye[5] proposed a potential which satisfies the following three conditions.

(i) At long distances, the $Q\bar{Q}$ potential grows linearly leading to confinement.

(ii) At short distances, the two-loop perturbative calculations of the $Q\bar{Q}$ potential give reliable predictions.

(iii) It should reproduce the $c\bar{c}$ and $b\bar{b}$ spectra.

The asymptotic behavior of the potential due to condition (ii) can be expressed in momentum space as

$$\tilde{V}(Q^2) = -\frac{4}{3}\frac{16\pi^2\rho(Q^2)}{Q^2} \tag{2.1}$$

with

$$\rho(Q^2) \underset{Q^2\to\infty}{\sim} \frac{1}{b_0 \ln(Q^2/\Lambda^2)} - \frac{b_1}{b_0^3}\frac{\ln\ln(Q^2/\Lambda^2)}{\ln^2(Q^2/\Lambda^2)} + O\left[\frac{1}{\ln^3(Q^2/\Lambda^2)}\right]. \tag{2.2}$$

Here $\ln(\Lambda/\Lambda_{\overline{\rm MS}}) = (31/3 - 10n_f/9)/(2b_0)$, and $b_0 = 25/3$, $b_1 = 154/3$ are the coefficients of the $\beta$ for four flavors. In coordinate space, it is equivalent to

$$V(r) = -\frac{16\pi}{25}\frac{1}{r\ln[1/(\Lambda_{\overline{\rm MS}}r)^2]} \times \left[1 + (2\gamma_E + \tfrac{53}{75})\frac{1}{\ln[1/(\Lambda_{\overline{\rm MS}}r)^2]} - \frac{462}{625}\frac{\ln\ln[1/(\Lambda_{\overline{\rm MS}}r)^2]}{\ln[1/(\Lambda_{\overline{\rm MS}}r)^2]}\right] + O\left[\frac{1}{\ln^3[1/(\Lambda_{\overline{\rm MS}}r)^2]}\right]. \tag{2.3}$$

 

Buchmüller and Tye found that $\rho(Q^2)$, as defined by the relation

$$\ln\frac{Q^2}{\Lambda^2}=\ln(e^{1/(b_0\rho)}-1)+\frac{b_1}{b_0{}^2}\left[\ln\frac{b_0}{l}-\gamma_E-\mathrm{Ei}(l\rho)\right], \tag{2.4}$$

satisfies the above three conditions. Here $\gamma_E$ is Euler's constant and $\mathrm{Ei}(x)$ the exponential integral.

Their potential, however, implies a fairly large $\Lambda_{\overline{\mathrm{MS}}}$ of about 500 MeV, which is related to the Regge slope parameter ($\alpha'\sim 1$ GeV$^{-2}$). It is not possible to incorporate a smaller $\Lambda_{\overline{\mathrm{MS}}}$ (down to 300 MeV) in this scheme to reproduce correct $c\bar{c}$ and $b\bar{b}$ spectra. Although they have an additional parameter $l$, this situation cannot be improved for any value of $l$. As another example they connected the short-range part of the potential with $\Lambda_{\overline{\mathrm{MS}}}=200$ MeV for $r<0.03$ fm, and the phenomenologically successful long-range part of the potential with $\Lambda_{\overline{\mathrm{MS}}}=500$ MeV for $r>0.1$ fm by logarithmic interpolation. If one connects the two potentials in this way, additional parameters become necessary. Furthermore, the potential is not smooth any more; hence it is not clear whether this potential really satisfies the above conditions (i), (ii), and (iii).

In order to overcome such problems, we propose here the following potential in coordinate space:

$$V(r)=V_{\mathrm{AF}}(r)+ar\ , \tag{2.5}$$

where

$$V_{\mathrm{AF}}(r)=-\frac{16\pi}{25}\frac{1}{rf(r)}\left[1+\frac{2\gamma_E+\frac{53}{75}}{f(r)}-\frac{462\ln f(r)}{625f(r)}\right] \tag{2.6}$$

with

$$f(r)=\ln[1/(\Lambda_{\overline{\mathrm{MS}}}r)^2+b]\ . \tag{2.7}$$

We call this potential "the potential $I$." The asymptotic-freedom potential $V_{\mathrm{AF}}(r)$ given in Eq. (2.5) satisfies the condition (ii) for small values of $r$ and becomes zero for large values of $r$. The linear-rising confining potential $ar$ is then added to $V_{\mathrm{AF}}(r)$.

While the Buchmüller-Tye potential has two free parameters $\Lambda_{\overline{\mathrm{MS}}}$ and $l$, we now have three parameters: $\Lambda_{\overline{\mathrm{MS}}}$, $a$, and $b$. The parameter $b$ is included to remove the singularity which comes from the inverse of the logarithmic function. In the Buchmüller-Tye potential[5] or Richardson potential,[12] a similar additional constant is added but they assumed that it is equal to 1. In some sense this is a parameter which is taken to be 1. One can easily prove that such an additional constant ($b$ in our case and 1 in the Buchmüller-Tye case) inside the logarithmic function does not change the short-range asymptotic behavior up to the order of $1/\ln^2(1/\Lambda_{\overline{\mathrm{MS}}}{}^2r^2)$ or $1/\ln^2(Q^2/\Lambda_{\overline{\mathrm{MS}}}{}^2)$.

Let us now find parameters $\Lambda_{\overline{\mathrm{MS}}}$, $a$, and $b$. We fix our parameters by minimizing the quantity

$$\chi^2\equiv\sum_{i=1}^{6}(m_i^{\mathrm{theory}}-m_i^{\mathrm{expt}})^2\ , \tag{2.8}$$

with $i=J/\psi$, $\psi(2S)$, $\psi(4S)$, $\Upsilon(1S)$, $\Upsilon(2S)$, $\Upsilon(3S)$. We do not include $\psi(3S)$ and $\Upsilon(4S)$ in our fit since masses of these states might be disturbed by some reason.[13] We have found that the $\chi^2$ value becomes a minimum for $\Lambda_{\overline{\mathrm{MS}}}=340$ MeV, but the other value, e.g., $\Lambda_{\overline{\mathrm{MS}}}=300$ MeV, is also acceptable. For example, we find an excellent fit by taking the following parameters:

$$\begin{aligned}&\Lambda_{\overline{\mathrm{MS}}}=300\text{ MeV},\quad a=0.1414\text{ GeV}^2,\quad b=19\ ,\\ &m_c=1.506\text{ GeV},\quad m_b=4.897\text{ GeV}\ .\end{aligned} \tag{2.9}$$

We call this potential the nonrelativistic version of the potential $I$. Note that $\Lambda_{\overline{\mathrm{MS}}}=300$ MeV is more reasonable than $\Lambda_{\overline{\mathrm{MS}}}=500$ MeV used by Buchmüller and Tye. In the potential $I$, the allowed range of $\Lambda_{\overline{\mathrm{MS}}}$ is $340\pm 50$ MeV. If we replace $ar$ by $a\sqrt{r}$ in Eq. (2.5) [i.e., $V(r)=V_{\mathrm{AF}}(r)+a\sqrt{r}$)], the allowed range of $\Lambda_{\overline{\mathrm{MS}}}$ becomes lower ($\Lambda_{\overline{\mathrm{MS}}}\sim 100\pm 50$ MeV).[6] In this case, however, we do not have the linear confining potential any more.

In order to extend the possible range of $\Lambda_{\overline{\mathrm{MS}}}$, keeping the linearly rising confining potential, we add a term which does not disturb either the short-range asymptotic behavior or the linear confining part of the potential,

$$V(r)=V_{\mathrm{AF}}(r)+dr\,e^{-gr}+ar\ . \tag{2.10}$$

In this case we can change $\Lambda_{\overline{\mathrm{MS}}}$ from 100 to 500 MeV keeping a good fit to the $c\bar{c}$ and $b\bar{b}$ spectra.

The potential with $b=20$ is called "the potential $J$" and the one with $b=5$ is called "the potential $K$." Instead of

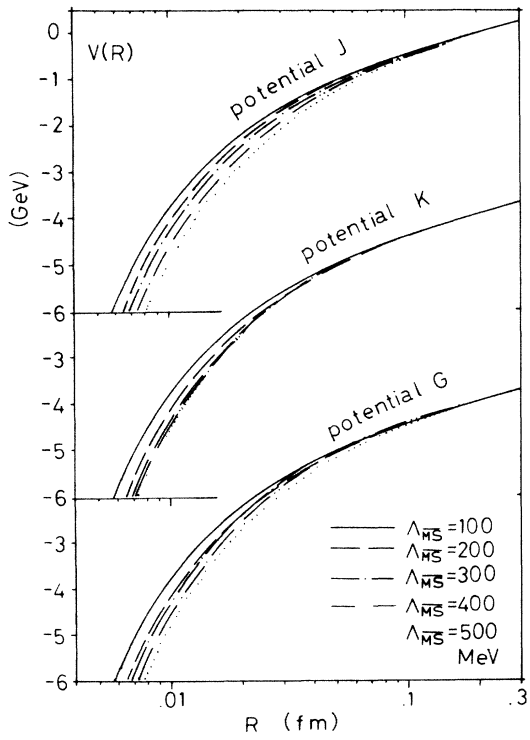


FIG. 1. Potentials $J$, $K$, and $G$ are plotted as a function of $R$ for $\Lambda_{\overline{\mathrm{MS}}}=100$, 200, 300, 400, and 500 MeV. A suitable constant is added to each potential so that all potentials take the same value at $R=0.3$ fm.

TABLE I. Parameters used for potentials (a) $J(b=20)$, (b) $K(b=5)$, and (c) $G(b=2)$. See Eqs. (2.7), (2.10), and (2.11).

| $\Lambda_{\overline{\rm MS}}$ (GeV) | $a$ (GeV$^2$) | $g$ (GeV) | $d$ (GeV$^2$) | $m_c$ (GeV) | $m_b$ (GeV) |
|---|---|---|---|---|---|
| | | (a) | | | |
| 0.1 | 0.1733 | 0.3076 | 0.4344 | 1.134 | 4.563 |
| 0.2 | 0.1587 | 0.3436 | 0.2550 | 1.322 | 4.731 |
| 0.3 | 0.1443 | 0.3280 | 0.0495 | 1.471 | 4.868 |
| 0.4 | 0.1387 | 2.903 | 0.582 | 1.515 | 4.910 |
| 0.5 | 0.1391 | 2.955 | 1.476 | 1.514 | 4.911 |
| | | (b) | | | |
| 0.1 | 0.1762 | 0.2753 | 0.4720 | 1.120 | 4.551 |
| 0.2 | 0.1734 | 0.3479 | 0.5362 | 1.267 | 4.684 |
| 0.3 | 0.1615 | 0.4482 | 0.6020 | 1.416 | 4.815 |
| 0.4 | 0.1389 | 0.6219 | 0.5632 | 1.604 | 4.986 |
| 0.5 | 0.1137 | 1.0029 | 0.7368 | 1.748 | 5.118 |
| | | (c) | | | |
| 0.1 | 0.1755 | 0.2849 | 0.421 | 1.125 | 4.553 |
| 0.2 | 0.1668 | 0.2948 | 0.352 | 1.264 | 4.679 |
| 0.3 | 0.0956 | 0.0993 | 0.1729 | 1.450 | 4.849 |
| 0.4 | 0.1375 | 0.2430 | 0.1311 | 1.535 | 4.924 |
| 0.5 | 0.1425 | 0.4275 | 0.1811 | 1.583 | 4.972 |

$f(r)=\ln[1/(\Lambda_{\overline{\rm MS}}r)^2+b]$ we have also tried another function, $f(r)=\ln[1/(\Lambda_{\overline{\rm MS}}r)+b]^2$, i.e.,

$$V(r)=V_{\rm AF}(r)+dr\,e^{-gr}+ar\ , \tag{2.11}$$

with $f(r)=\ln[1/(\Lambda_{\overline{\rm MS}}r)+b]^2$. This is called "the potential $G$."

Parameters of the potentials $J$, $K$, and $G$, their predictions for $c\bar{c}$ and $b\bar{b}$ spectra, and their shapes are shown in Tables I and II, and Fig. 1, respectively. We find reasonable fits for all these potentials from $\Lambda_{\overline{\rm MS}}=0.1$ GeV to $\Lambda_{\overline{\rm MS}}=0.5$ GeV. Small discrepancies between the theory and experiment can be seen, e.g., for $\psi(3S)$, $\psi(1D)$, and $\psi(4S)$. We do not take these seriously since similar discrepancies are seen for any potential model and it might be related to the threshold effects[14] or $Q\bar{Q}g$-$Q\bar{Q}$ mixing.[13]

TABLE II. The $c\bar{c}$ and $b\bar{b}$ spectra predicted by potentials $J$, $K$, and $G$. The difference $E$(theory) $-$ $E$(experiment) is listed in MeV. (a) Nonrelativistic model with parameters (2.9). (b) Relativistic model with parameters (3.2).

| | | | Potential | $I$ | | | | | | | | | | | | | | | |
|---|---|---|---|---|---|---|---|---|---|---|---|---|---|---|---|---|---|---|---|
| | | (GeV) | (a) | (b) | Potential $J$ | | | | | Potential $K$ | | | | | Potential $G$ | | | | |
| $c\bar{c}$ | Expt | $\Lambda_{\overline{\rm MS}}$ | 0.3 | 0.3 | 0.1 | 0.2 | 0.3 | 0.4 | 0.5 | 0.1 | 0.2 | 0.3 | 0.4 | 0.5 | 0.1 | 0.2 | 0.3 | 0.4 | 0.5 |
| $1S$ | 3096 | | −3 | 0 | −3 | −2 | −4 | 1 | 1 | −2 | −7 | −1 | −3 | −2 | 1 | −1 | −18 | −4 | −3 |
| $1P$ | 3521 | | −10 | 13 | 5 | 2 | −3 | 0 | −1 | 4 | −6 | 4 | 1 | 2 | 6 | 3 | −12 | −5 | −1 |
| $1D$ | 3772 | | 23 | | 37 | 34 | 31 | 31 | 30 | 35 | 28 | 35 | 34 | 40 | 37 | 36 | 42 | 36 | 33 |
| $2S$ | 3685 | | −3 | 0 | 5 | 2 | 1 | 0 | 0 | 3 | −1 | 3 | 4 | 11 | 5 | 5 | 17 | 9 | 2 |
| $3S$ | 4030 | | 55 | 56 | 48 | 49 | 56 | 54 | 54 | 47 | 48 | 46 | 52 | 60 | 48 | 50 | 77 | 61 | 55 |
| $2D$ | 4159 | | 0 | | −5 | −4 | 3 | 2 | 2 | −6 | −6 | −7 | −2 | 5 | −5 | −4 | 19 | 5 | 3 |
| $4S$ | 4415 | | 5 | 2 | 3 | −1 | 5 | 0 | 1 | 0 | 6 | 0 | 0 | −9 | 1 | −2 | −4 | −2 | 3 |
| $b\bar{b}$ | Expt | | | | | | | | | | | | | | | | | | |
| $1S$ | 9460 | | 9 | 0 | 0 | 1 | −1 | 0 | 0 | 0 | 5 | 0 | 2 | 1 | 1 | 2 | 9 | 8 | −2 |
| $1P$ | 9898 | | −18 | −7 | −20 | −17 | −12 | −1 | 4 | −18 | −16 | −18 | −24 | −25 | −19 | −14 | −32 | −20 | −7 |
| $2S$ | 10023 | | −6 | −1 | 5 | 5 | 1 | 4 | 2 | 5 | 0 | 4 | 2 | 0 | 4 | 4 | −11 | −6 | 1 |
| $3S$ | 10355 | | −12 | 4 | −3 | −4 | −4 | −1 | −1 | −5 | −6 | −4 | −4 | 2 | −7 | −3 | 5 | −2 | 0 |
| $4S$ | 10573 | | 24 | 51 | 14 | 21 | 31 | 34 | 36 | 13 | 18 | 19 | 28 | 41 | 10 | 20 | 53 | 37 | 37 |
| $5S$ | 10868? | | −52 | −17 | −81 | −66 | −47 | −44 | −42 | −83 | −69 | −66 | −51 | −37 | −86 | −70 | −25 | −43 | −40 |
| $6S$ | 11019? | | −6 | 36 | −50 | −28 | −4 | 0 | 2 | −52 | −30 | −24 | −5 | 4 | −55 | −35 | 8 | −3 | 6 |
| $2P$ | 10259 | | −21 | −3 | −9 | −10 | −11 | −5 | −1 | −10 | −12 | −7 | −11 | −11 | −12 | −8 | −12 | −12 | −4 |

The slope parameter found in these fits is around 0.15 $GeV^2$. The quark masses $m_c$ and $m_b$ increase as the values of $\Lambda_{\overline{MS}}$ increase. This is explained in the following way. We have assumed the short-range asymptotic behavior given by Eq. (2.3). The absolute value of this short-range potential decreases with increasing $\Lambda_{\overline{MS}}$. In order to reproduce experimental masses we need larger quark masses for larger values of $\Lambda_{\overline{MS}}$. This situation becomes completely different if we are allowed to add an additional constant to Eq. (2.3). However, we have not attempted such a possibility in this paper.

## III. THE RELATIVISTIC POTENTIAL MODEL

In order to study the relativistic effects to heavy-quarkonium spectra we use the Salpeter equation

$$[(-\nabla^2+m_q^2)^{1/2}+(-\nabla^2+m_{\bar{q}}^2)^{1/2}+V(r)]\psi=E\psi\ . \quad (3.1)$$

We solve this equation numerically, using the program developed by Nickisch, Durand, and Durand.[15] We first try to find a potential which reproduces $c\bar{c}$ and $b\bar{b}$ spectra. We again use the potential $I$ defined by Eqs. (2.5) and (2.6), but with different parameters:

$$\Lambda_{\overline{MS}}=300\ \text{MeV},\ a=0.1585\ \text{GeV}^2\ ,$$
$$b=23.3,\ m_c=1.494\ \text{GeV},\ m_b=4.874\ \text{GeV}\ . \quad (3.2)$$

These parameters should be compared with the nonrelativistic ones, Eq. (2.9). We now have a slightly larger slope than the nonrelativistic one (see Fig. 2). This can be understood in the following way. In the nonrelativistic models the kinetic energy $p^2/2m$ is overestimated compared with $(p^2+m^2)^{1/2}-m$. Thus if we must fit the same $c\bar{c}$ and $b\bar{b}$ spectra in both the nonrelativistic and relativistic models, we need a smaller slope to absorb the overestimation in the kinetic term in the nonrelativistic model than in the relativistic model.

We find again a reasonable fit with the parameter (3.2) (see Table II). These calculations are performed by making use of the method by Nickish, Durand, and Durand with $N=77$, which is fast and accurate. The accuracy of this calculation is discussed in Ref. 15.

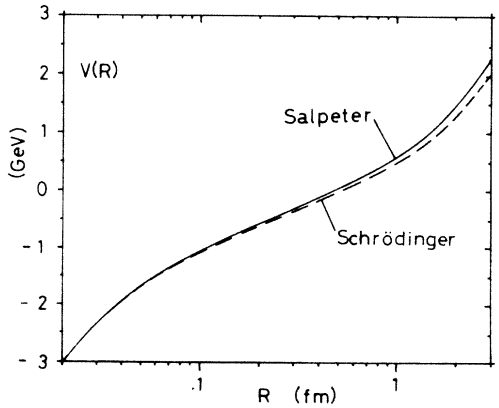


FIG. 2. Potentials for the Schrödinger equation and for the Salpeter equation. $\Lambda_{\overline{MS}}=300$ MeV is assumed.

## IV. $t$-QUARKONIUM SPECTROSCOPY AND $\Lambda_{\overline{MS}}$

In order to predict the properties of $t\bar{t}$ states, there are various theoretical ambiguities. Even if we assume the flavor independence of the quarkonium potential, the short-range behavior ($r\lesssim 0.1$ fm) is undetermined from the $c\bar{c}$ and $b\bar{b}$ spectra alone. Such a short-range behavior becomes especially important for the $1S$ $t\bar{t}$ state. The QCD predicts the short-range behavior but the scale parameter $\Lambda_{\overline{MS}}$ must be determined experimentally.

Buchmüller and Tye[5] studied the $t\bar{t}$ spectroscopy by the use of their potential for various values of $\Lambda_{\overline{MS}}$. We will

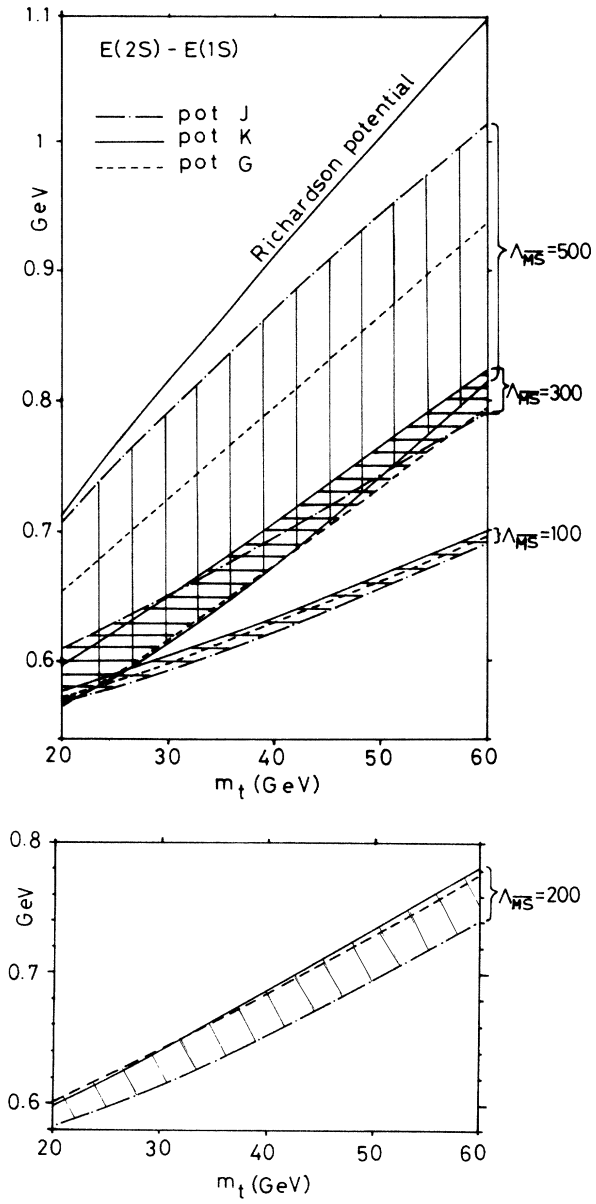


FIG. 3. $t$-quarkonium mass difference $E(2S)-E(1S)$ as a function of the top-quark mass for various $\Lambda_{\overline{MS}}$. Results for the potentials $J$, $K$, and $G$ and for the Richardson potential are shown. Shaded regions correspond to the allowed region for various $\Lambda_{\overline{MS}}$. These regions should be regarded as theoretical ambiguities.

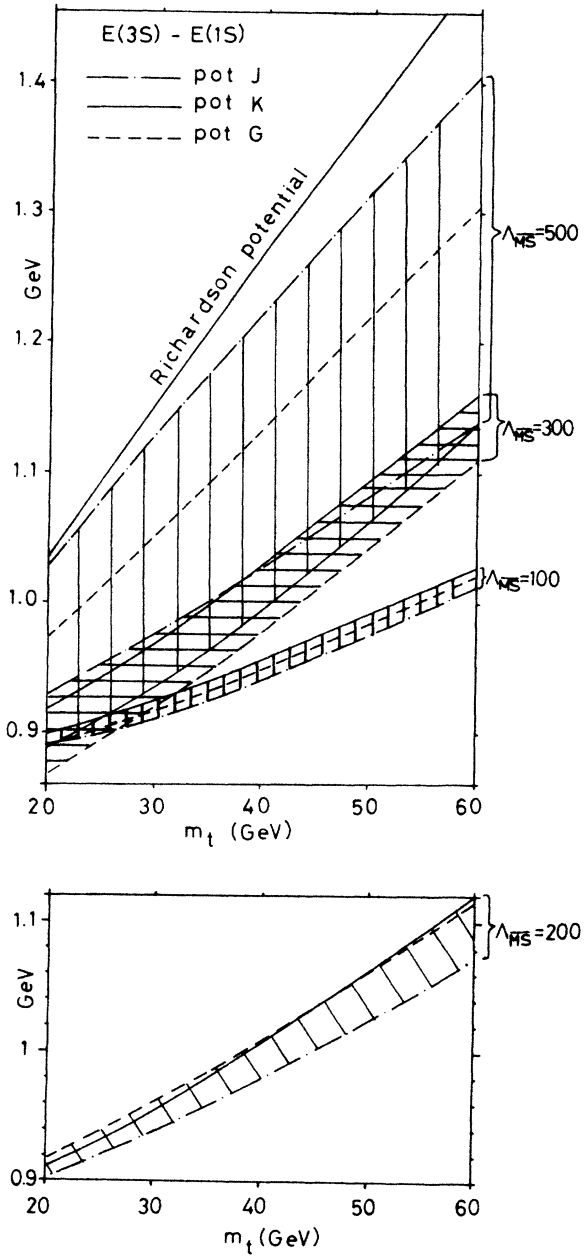


FIG. 4. Same as Fig. 3 but for $E(3S)-E(1S)$.

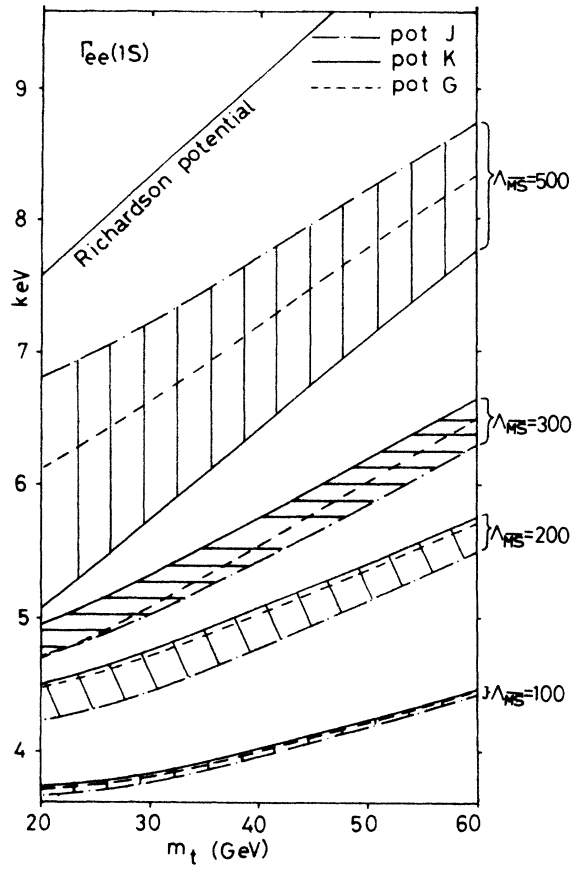


FIG. 5. Same as Fig. 3 but for $\Gamma_{ee}(1S)$. The QCD correction factor $1-16\alpha_S/3\pi$ ($\sim$0.9) and $Z^0$ boson effects are omitted.

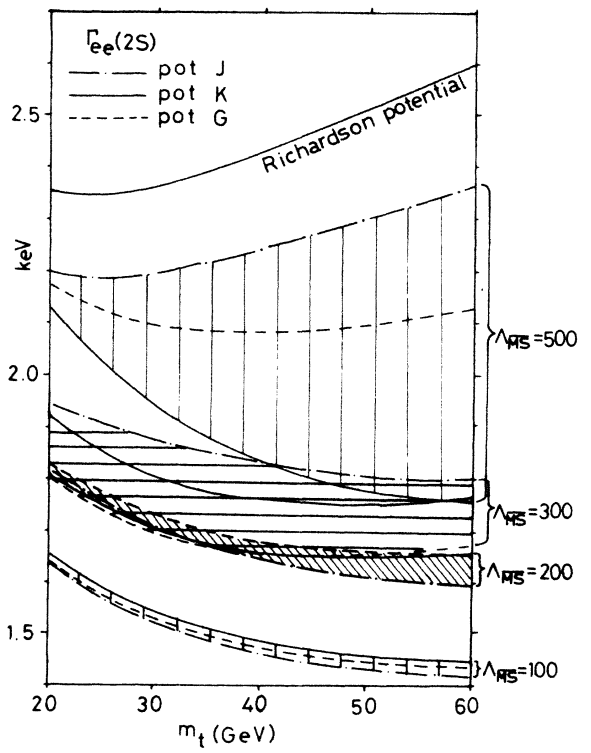


FIG. 6. Same as Fig. 5 but for $\Gamma_{ee}(2S)$.

recalculate the properties of the $t\bar{t}$ spectra in a similar line with the following improvements.

(i) The short-range asymptotic behavior of the potential is smoothly interpolated to the long-range linearly rising confining part.

(ii) For each value of $\Lambda_{\overline{MS}}$ we have made the $\chi^2$ fit to the $c\bar{c}$ and $b\bar{b}$ spectra. In this sense our parameters are chosen without any prejudice for each $\Lambda_{\overline{MS}}$.

(iii) We study three kinds of potentials for each $\Lambda_{\overline{MS}}$, and hence, not only the $\Lambda_{\overline{MS}}$ dependence, but also the potential dependence of various properties of $t\bar{t}$ can be studied.

(iv) All our potentials can be generated easily, so that anyone can reproduce our results without any trouble.

(v) We also check the relativistic effects by solving the Salpeter equation.

### A. $\Lambda_{\overline{\rm MS}}$ and potential dependence of the properties of $t\bar{t}$ states

Using the potentials $J$, $K$, and $G$ we compute properties of the $t\bar{t}$ states. The quantities $E(2S)-E(1S)$, $E(3S)-E(1S)$, $\Gamma_{ee}(1S)$, and $\Gamma_{ee}(2S)$ are plotted in Figs. 3–6, respectively. The Schrödinger equation is used in this computation. For $\Gamma_{ee}$ we use the well-known formula[16]

$$\Gamma_{ee}=\frac{4\alpha^2 e_Q{}^2 R(0)^2}{M(t\bar{t})^2} \tag{4.1}$$

with $e_Q=\frac{2}{3}$. The QCD correction factor $1-16\alpha_S/3\pi$ ($\sim 0.9$) and $Z^0$-boson effects are omitted. One can easily include them, but we omit them here for simplicity.

From Figs. 3–6 we can reach the following conclusions.

(i) The mass difference between the $1S$ and $2S$ states tends to become larger with increasing $\Lambda_{\overline{\rm MS}}$. This tendency becomes larger for larger values of $m_t$.

(ii) The shaded regions correspond to the allowed regions for $\Lambda_{\overline{\rm MS}}=100$, 200, 300, and 500 MeV, respectively. The region where the potential can be determined by the QCD decreases as $\Lambda_{\overline{\rm MS}}$ increases. Thus, for large $\Lambda_{\overline{\rm MS}}$ an undetermined gap appears between the phenomenologically fixed region (0.1–1 fm) and the one fixed by the QCD. Thus, the shaded region becomes broader as $\Lambda_{\overline{\rm MS}}$ increases.

(iii) The predictions by the Richardson potential are also added in Figs. 3–6. One can see that the Richardson potential has a more singular short-range behavior than the one with $\Lambda_{\overline{\rm MS}}=500$ MeV.

(iv) Ambiguities coming from potentials are larger for level splittings $[E(2S)-E(1S),\ E(3S)-E(1S)]$ than those for the leptonic widths $\Gamma_{ee}$.

### B. Use of the Salpeter equation to study the relativistic effects for properties of $t\bar{t}$

The $t$ quark inside the $t$-quarkonium system is moving nonrelativistically ($v^2/c^2\sim 0.01$ for $m_t=40$ GeV). Thus, the $t$-quarkonium system can be well described by the nonrelativistic Schrödinger equation. However, the $c\bar{c}$ and $b\bar{b}$ systems are not so nonrelativistic and if the potential is fixed by a fit to $c\bar{c}$ and $b\bar{b}$ spectra we find the steeper potential for the relativistic model than for the nonrelativistic model. Thus, the relativistic model predicts larger spacings between various excited levels of

TABLE III. Energy level (in MeV) and $\Gamma_{ee}$ (in keV) of $t\bar{t}$ states predicted by the Schrödinger theory and Salpeter theory. The potential $I$ [Eqs. (2.5)–(2.7)] with parameters (2.9) and (3.2) is used.

| | | Schrödinger theory | | | Salpeter theory | | |
|---|---|---|---|---|---|---|---|
| $E_{(n+1)S}-E_{nS}$ | $m_t$ (GeV) | 30 | 40 | 50 | 30 | 40 | 50 |
| $E(2S)-E(1S)$ | | 624 | 658 | 686 | 657 | 703 | 751 |
| $E(3S)-E(2S)$ | | 315 | 322 | 329 | 325 | 334 | 342 |
| $E(4S)-E(3S)$ | | 214 | 216 | 218 | 221 | 222 | 225 |
| $E(5S)-E(4S)$ | | 167 | 165 | 165 | 172 | 170 | 170 |
| $E(6S)-E(5S)$ | | 140 | 137 | 135 | 145 | 141 | 139 |
| $E(7S)-E(6S)$ | | 123 | 118 | 116 | 128 | 123 | 120 |
| $E(8S)-E(7S)$ | | 111 | 106 | 103 | 116 | 111 | 108 |
| $E(9S)-E(8S)$ | | 102 | 97 | 94 | 108 | 102 | 98 |
| $E(10S)-E(9S)$ | | 96 | 90 | 87 | 101 | 95 | 91 |
| $E(11S)-E(10S)$ | | 90 | 85 | 81 | 95 | 89 | 85 |
| $E(12S)-E(11S)$ | | 86 | 81 | 77 | 90 | 84 | 80 |
| | | Schrödinger theory | | | Salpeter theory | | |
| $\Gamma_{ee}$ (keV) | $m_t$ (GeV) | 30 | 40 | 50 | 30 | 40 | 50 |
| $\Gamma_{ee}(1S)$ | | 5.03 | 5.56 | 6.46 | 6.21 | 6.63 | 7.10 |
| $\Gamma_{ee}(2S)$ | | 1.80 | 1.77 | 1.76 | 2.36 | 2.30 | 2.26 |
| $\Gamma_{ee}(3S)$ | | 1.13 | 1.09 | 1.07 | 1.47 | 1.40 | 1.36 |
| $\Gamma_{ee}(4S)$ | | 0.84 | 0.79 | 0.77 | 1.11 | 1.03 | 0.98 |
| $\Gamma_{ee}(5S)$ | | 0.68 | 0.63 | 0.60 | 0.91 | 0.83 | 0.79 |
| $\Gamma_{ee}(6S)$ | | 0.59 | 0.54 | 0.50 | 0.80 | 0.71 | 0.67 |
| $\Gamma_{ee}(7S)$ | | 0.53 | 0.47 | 0.44 | 0.72 | 0.64 | 0.59 |
| $\Gamma_{ee}(8s)$ | | 0.48 | 0.43 | 0.40 | 0.67 | 0.59 | 0.54 |
| $\Gamma_{ee}(9S)$ | | 0.45 | 0.40 | 0.36 | 0.62 | 0.55 | 0.49 |
| $\Gamma_{ee}(10S)$ | | 0.43 | 0.37 | 0.34 | 0.59 | 0.51 | 0.46 |
| $\Gamma_{ee}(11S)$ | | 0.41 | 0.36 | 0.32 | 0.56 | 0.48 | 0.44 |
| $\Gamma_{ee}(12S)$ | | 0.39 | 0.34 | 0.31 | 0.53 | 0.46 | 0.42 |

$t\bar{t}$ than the nonrelativistic model by around 5% and the former predicts larger $\Gamma_{ee}$ than the latter by around 10–30%. These are shown in Table III.

## V. SPIN-DEPENDENT FORCES AND $\Lambda_{\overline{\rm MS}}$

In this section we show that the fine and hyperfine splittings are very sensitive to the value of $\Lambda_{\overline{\rm MS}}$; thus the allowed range of $\Lambda_{\overline{\rm MS}}$ might be restricted from the data of already known quarkonia, i.e., $c\bar{c}$ and $b\bar{b}$. The QCD radiative corrections to the spin-dependent forces have already been calculated by various authors.[17–19] Taking here the scheme by Gupta, Radford, and Repko,[18] we compute the $\Lambda_{\overline{\rm MS}}$ dependence of spin-dependent forces. The interactions are given by[18]

$$H_{SS}=\frac{8\pi\alpha_S}{9m^2}\sigma_1\cdot\sigma_2\left[\left[1-\frac{\alpha_S}{12\pi}(26+9\ln 2)\right]\delta(\mathbf{r})-\frac{\alpha_S}{24\pi^2}(33-2n_f)\nabla^2\left[\frac{\ln(\mu r)+\gamma_E}{r}\right]+\frac{21\alpha_S}{16\pi^2}\nabla^2\left[\frac{\ln(mr)+\gamma_E}{r}\right]\right]$$

$$\equiv c\sigma_1\cdot\sigma_2\ , \tag{5.1}$$

$$H_T=\frac{\alpha_S}{3m^2}\frac{3\sigma_1\cdot\hat{\mathbf{r}}\sigma_2\cdot\hat{\mathbf{r}}-\sigma_1\cdot\sigma_2}{r^3}\left[1+\frac{4\alpha_S}{3\pi}+\frac{\alpha_S}{6\pi}(33-2n_f)[\ln(\mu r)+\gamma_E-\tfrac{4}{3}]-\frac{3\alpha_S}{\pi}[\ln(mr)+\gamma_E-\tfrac{4}{3}]\right]$$

$$\equiv B(3\sigma_1\cdot\hat{\mathbf{r}}\sigma_2\cdot\hat{\mathbf{r}}-\sigma_1\cdot\sigma_2)\ , \tag{5.2}$$

$$H_{LS}=\frac{2\alpha_S}{m^2}\frac{\mathbf{L}\cdot\mathbf{S}}{r^3}\left[1-\frac{11\alpha_S}{18\pi}+\frac{\alpha_S}{6\pi}(33-2n_f)[\ln(\mu r)+\gamma_E-1]-\frac{2\alpha_S}{\pi}[\ln(mr)+\gamma_E-1]\right]-\frac{a}{2m^2}\frac{\mathbf{L}\cdot\mathbf{S}}{r}$$

$$\equiv A\mathbf{L}\cdot\mathbf{S}\ , \tag{5.3}$$

where $m$ is the quark mass, $a$ is the slope of the scalar confining potential, and $\mu$ is the renormalization scale.

These interactions depend not only on the renormalization scheme, but also on the renormalization scale. We take the renormalization scheme by Gupta and Radford[20] and choose $\mu$ so as to minimize the effect of higher-order terms which would be generated by the renormalization-group improvement of the potential. These terms involve higher powers of

$$\frac{\alpha_S}{12\pi}(33-2n_f)\frac{\mathbf{k}^2}{\mu^2} \tag{5.4}$$

whose expectation value is not very sensitive to the variations in $\mu$ except for the $S$ state.

We fix $\mu$ so that the quantity

$$\xi=(\alpha_S/12\pi)(33-2n_f)\langle\ln(\mathbf{k}^2/\mu^2)\rangle/\langle 1\rangle$$
$$=\frac{\alpha_S(33-2n_f)}{24\pi^2|\psi(0)|^2}\int d\mathbf{r}\frac{\ln(\mu r)+\gamma_E}{r}\nabla^2[\psi^*(r)\psi(r)] \tag{5.5}$$

becomes small for all $S$ states, where $\langle 1\rangle\equiv|\psi(0)|^2$. In our calculation we find $\mu$ which minimizes the quantity

$$\chi^2\equiv\xi_{1S}{}^2+\xi_{2S}{}^2+\xi_{3S}{}^2+\xi_{4S}{}^2\ . \tag{5.6}$$

The scale parameter in the Gupta-Radford (GR) renormalization scheme is related to $\Lambda_{\overline{\rm MS}}$ by

$$\Lambda_{\rm GR}=\Lambda_{\overline{\rm MS}}\exp\left[\frac{6\lambda}{33-2n_f}\right] \tag{5.7}$$

with $\lambda=(49-10n_f/3)/12$. The coupling constant is given by

$$\alpha_S=-\frac{6\pi}{(33-2n_f)\ln\Lambda_{\rm GR}/\mu}\ . \tag{5.8}$$

Assuming the $n_f=4$ and using the potentials $J$ and $K$ (nonrelativistic wave functions), we compute expectation values of the spin-dependent potentials $(H_{SS},H_{LS},H_T)$. Results are shown in Table IV. We conclude with the following remarks.

(i) The fine and hyperfine splittings are not very sensitive to the choice of potentials, but rapidly increase as $\Lambda_{\overline{\rm MS}}$ increases.

(ii) For $\Lambda_{\overline{\rm MS}}\sim 200$ MeV, we can reproduce approximately all hyperfine and fine splittings of $c\bar{c}$ and $b\bar{b}$ states. The values $\Lambda_{\overline{\rm MS}}=400$ and 500 MeV are completely ruled out. This conclusion does not depend on the choice of potentials.

(iii) Gupta, Radford, and Repko[18] found the following parameters: $\Lambda_{\overline{\rm MS}}=134$ MeV ($n_f=4$), $\mu=1.88$ GeV for $m_c=1.2$ GeV, $\mu=3.75$ GeV for $m_b=4.87$ GeV, which are not very far from ours.

## VI. SUMMARY AND CONCLUSIONS

We have found the $Q\bar{Q}$ potentials which reproduce the properties of $c\bar{c}$ and $b\bar{b}$ states for various values of $\Lambda_{\overline{\rm MS}}$. These potentials have linearly rising confining parts and a short-range asymptotic behavior calculated to the fourth order in perturbative QCD.

Using the nonrelativistic wave equations, we have fixed acceptable parameters for $\Lambda_{\overline{\rm MS}}=100$, 200, 300, 400, and 500 MeV. We have then computed various properties of $t$-quarkonium states as a function of $\Lambda_{\overline{\rm MS}}$ from these potentials. We have shown that the ambiguities coming from the shape of the potential are large, especially for

TABLE IV. The hyperfine and fine splittings in MeV for various $\Lambda_{\overline{\rm MS}}$ predicted by the potentials $J$ and $K$. The scheme by Gupta, Radford, and Repko (Ref. 18) is used.

| $c\bar{c}$ | | $S$ state $^3S_1$-$^1S_0$ | | $1P$ state | | | |
|---|---|---|---|---|---|---|---|
| | Expt | $1S$ | $2S$ | $A$ | $B$ | $\mu$ (GeV) | $\alpha_S$ |
| $\Lambda_{\overline{\rm MS}}$ (MeV) | | 116±6 | 95 | 34.9±0.6 | 10.0±0.3 | | |
| pot $J$ | 100 | 117 | 68 | 20.8 | 8.0 | 1.80 | 0.346 |
| | 200 | 140 | 84 | 40.5 | 10.9 | 1.98 | 0.477 |
| | 300 | 160 | 101 | 57.9 | 13.9 | 2.14 | 0.603 |
| | 400 | 195 | 125 | 79.6 | 18.4 | 2.60 | 0.752 |
| | 500 | 245 | 162 | 112 | 25.6 | 3.85 | 0.939 |
| pot $K$ | 100 | 118 | 69 | 20.3 | 8.0 | 1.79 | 0.347 |
| | 200 | 146 | 90 | 40.3 | 11.4 | 1.96 | 0.481 |
| | 300 | 167 | 100 | 59.5 | 14.7 | 2.09 | 0.614 |
| | 400 | 165 | 102 | 77.6 | 17.9 | 2.23 | 0.750 |
| | 500 | 163 | 108 | 99.6 | 22.2 | 2.34 | 0.908 |

| $b\bar{b}$ | | $^3S_1$-$^1S_0$ | | $1P$ state | | $2P$ state | | | |
|---|---|---|---|---|---|---|---|---|---|
| | | $1S$ | $2S$ | $A$ | $B$ | $A$ | $B$ | $\mu$ (GeV) | $\alpha_S$ |
| | Expt | | | 14.2±0.3 | 3.1±0.2 | | | | |
| $\Lambda_{\overline{\rm MS}}$ (MeV) | | | | 13±1 | 2.5±0.3 | 11±2 | 1.7±1.0 | | |
| pot $J$ | 100 | 33.5 | 18.5 | 10.3 | 2.27 | 6.77 | 1.52 | 3.85 | 0.257 |
| | 200 | 39.5 | 21.5 | 14.3 | 2.94 | 9.38 | 1.98 | 4.07 | 0.328 |
| | 300 | 44.6 | 23.4 | 17.6 | 3.51 | 12.0 | 2.46 | 4.25 | 0.389 |
| | 400 | 52.7 | 26.5 | 21.1 | 4.15 | 14.5 | 2.94 | 4.43 | 0.446 |
| | 500 | 61.6 | 30.6 | 24.5 | 4.79 | 17.1 | 3.46 | 4.61 | 0.500 |
| pot $K$ | 100 | 34.2 | 18.6 | 10.3 | 2.27 | 6.76 | 1.53 | 3.86 | 0.257 |
| | 200 | 41.0 | 22.4 | 13.7 | 2.87 | 9.38 | 2.01 | 4.09 | 0.327 |
| | 300 | 44.4 | 25.0 | 17.6 | 3.55 | 11.5 | 2.39 | 4.25 | 0.389 |
| | 400 | 42.1 | 24.8 | 20.8 | 4.09 | 13.6 | 2.74 | 4.36 | 0.450 |
| | 500 | 41.0 | 24.4 | 24.3 | 4.68 | 16.3 | 3.24 | 4.48 | 0.510 |

$\Lambda_{\overline{\rm MS}} > 300$ MeV, but decrease for small values of $\Lambda_{\overline{\rm MS}}$. If $\Lambda_{\overline{\rm MS}}$ is as small as 100 MeV, the $t$-quarkonium properties can be almost uniquely determined.

We have also computed the fine and hyperfine splittings of $c\bar{c}$ and $b\bar{b}$ states. These splittings rapidly increase as $\Lambda_{\overline{\rm MS}}$ increases. Experimental $c\bar{c}$ and $b\bar{b}$ splittings can be reproduced for $\Lambda_{\overline{\rm MS}} \sim 200$ MeV while $\Lambda_{\overline{\rm MS}} = 400$ and 500 MeV are clearly ruled out.

Taking the preferred value $\Lambda_{\overline{\rm MS}} = 200$ MeV, we can predict

$$E(2S) - E(1S) = 670 \pm 15 \text{ MeV},$$

$$E(3S) - E(1S) = 995 \pm 15 \text{ MeV},$$

$$E(4S) - E(1S) = 1220 \pm 15 \text{ MeV}$$

for $m_t = 40$ GeV.

We have also studied how the results are affected if the Schrödinger equation is replaced by the Salpeter equation which has a relativistic kinematic part $(p^2+m^2)^{1/2}-m$. We find that $E((n+1)S)-E(nS)$ increases around 5% and $\Gamma_{ee}(nS)$ increases 10—30% for $n$ up to 10.

## ACKNOWLEDGMENTS

We would like to thank Professor L. Durand for allowing us to use the computer program to solve the Salpeter equation (Ref. 15) and for helpful communications. We would also like to thank Dr. T. Yoshino, Dr. S. Yazaki, and Dr. F. Schöberl for discussions. One of the authors (S.O.) is grateful to Soryushi Shogakukai for financial support. The computer calculation for this work has been financially supported in part by the Institute for Nuclear Study, University of Tokyo.

*Present address: Physics Department, University of Tokyo, Tokyo 113, Japan.

[1]Particle Data Group, C. G. Wohl *et al.*, Rev. Mod. Phys. **56**, S1 (1984).

[2]K. Berkelman, Cornell University Report No. CLNS-85/649, 1985 (unpublished).

[3]G. Arnison *et al.*, Phys. Lett. **147B**, 493 (1984).

[4]H. Krasemann and S. Ono, Nucl. Phys. **B154**, 283 (1979).

[5]W. Buchmüller and S.-H. H. Tye, Phys. Rev. D **24**, 132 (1982); W. Buchmüller, G. Grunberg, and S.-H. H. Tye, Phys. Rev.

Lett. **45**, 103 (1980).
[6]J. H. Kühn and S. Ono, Z. Phys. C **21**, 395 (1984).
[7]E. Eichten, in *The Sixth Quark,* proceedings of the Twelfth SLAC Summer Institute on Particle Physics, 1984, edited by P. M. McDonough (SLAC, Stanford, California, 1985).
[8]S. Gusken, J. H. Kühn, and P. M. Zerwas, Nucl. Phys. **B262**,393 (1985); W. Buchmüller *et al.*, Report No. MPI-PAE/PTh 85/85 CERN 86-02 (unpublished).
[9]K. Igi and K. Hikasa, Phys. Rev. D **28**, 565 (1983).
[10]J. Morishita *et al.*, Z. Phys. C **19**, 167 (1983).
[11]O. Abe *et al.*, Phys. Rev. D **27**, 675 (1983).
[12]J. L. Richardson, Phys. Lett. **82B**, 272 (1979).
[13]S. Ono, Z. Phys. C **26**, 307 (1985); Phys. Rev. D **33**, 2660 (1986).
[14]K. Heikkilä, N. A. Törnqvist, and S. Ono, Phys. Rev. D **29**, 110 (1984); **29**, 2136(E) (1984); N. A. Törnqvist, Phys. Rev. Lett. **53**, 878 (1985).
[15]L. J. Nickisch, L. Durand, and B. Durand, Phys. Rev. D **30**, 660 (1984).
[16]V. A. Mateev, B. V. Struminskii, and A. N. Tavkhelidze, DUBNA Report No. P-2524, 1965 (unpublished); H. Pietschmann and W. Thirring, Phys. Lett. **21**, 713 (1966); R. van Royen and V. F. Weisskopf, Nuovo Cimento **50**, 617 (1967).
[17]W. Buchmüller, Y. J. Ng, and S.-H. H. Tye, Phys. Rev. D **24**, 3003 (1981); J. Pantaleone, S.-H. H. Tye, and Y. J. Ng, *ibid.* D **33**, 777 (1986).
[18]S. N. Gupta, S. F. Radford, and W. W. Repko, Phys. Rev. D **26**, 3305 (1982); S. N. Gupta and S. F. Radford, *ibid.* **25**, 3430 (1982).
[19]T. W. Kephart, Y. J. Ng, and H. Van Dam, Phys. Rev. D **26**, 3260 (1982).
[20]S. N. Gupta and S. F. Radford, Phys. Rev. D **25**, 2690 (1982).